

# A Novel Autocorrelation Method for Measuring the Thickness Anisotropy Tensor of Trabecular Bone

B. Vasilic<sup>1</sup>, F. W. Wehrli<sup>1</sup>

<sup>1</sup>Laboratory for Structural NMR Imaging, Department of Radiology, University of Pennsylvania Medical Center, Philadelphia, PA, United States

## INTRODUCTION

Trabecular bone (TB) micro-structure is inherently anisotropic, which is a consequence of Wolff's law [1]. It is well known that trabeculae transverse to the main loading direction are lost preferentially during aging. Therefore, mean trabecular thickness and its spatial anisotropy are relevant to the bone's mechanical behavior. Measuring these parameters in-vivo by micro-MRI is a challenging goal not yet achieved with accuracy sufficient to detect changes in individual subjects. TB is a quasi-periodic structure so its autocorrelation function (ACF) carries information about the TB thickness and spacing [2], as well as their dependence on orientation. The full width at half maximum (FWHM) of the ACF, along a given direction, can be used as an estimate of TB thickness in that direction. Using the Wiener-Khinchine theorem [3], the ACF can be calculated directly from  $k$ -space data acquired in standard, rectilinear MRI. Here we focus on the anisotropy tensor describing TB thickness along different directions as estimated by the FWHM of the ACF. We show that by selective, anisotropic sampling only along the principal directions, one can quickly and with high precision estimate the principal values of the TB thickness anisotropy tensor. The principal directions can be determined from short, low resolution scans.

## THEORY AND METHODS

Let us examine the behavior of the ACF when its Fourier transform (FT) is sampled on an anisotropic grid. For simplicity, we will consider only the two-dimensional (2-D) case. To this end we discretely sample the analytic FTs of two ACFs - a product of two Lorentzians and a product of two Gaussians,  $f_x(x)f_y(y)$ , as shown in Figs. 1a) and b). These two functions represent two extremes - the Lorentzian product has a FWHM that varies sharply with orientation while the Gaussian product varies more smoothly with its direction. The FWHM of the ACFs was chosen to be  $2(4)$  along the  $x(y)$  direction measured in arbitrary units. This choice produces an anisotropy tensor of the FWHM with principal axes parallel to the coordinate axes and principal values of 2 and 4 as shown in Figs. 1c) and d).

The FT of each ACF was first sampled on an isotropic grid of  $128 \times 128$  points with a field of view of  $128 \times 128$  units, resulting in a voxel size of  $1 \times 1$ . This choice is realistic for our application where individual trabeculae cover only a few voxels. The resulting ACFs obtained from inverting the discrete FT, Figs. 1a) and b), were then sampled along 360 directions spaced by  $1^\circ$ . The FWHM was determined along each of these directions (FWHM directions, for brevity). The resulting angular dependence of FWHM is shown in Figs. 1c) and d). This estimate of the FWHM was taken as the gold standard (inner solid line in Figs. 1c) and d)).

We then sampled a rotated FT of the ACF on the same  $128 \times 128$  grid. This was done for 36 angles,  $\alpha$ , spaced by  $5^\circ$  using analytic formulas for the FT of a Lorentzian and a Gaussian. The resolution in the  $y$  direction was then reduced by filling with zeros portions of  $k$ -space for which  $|k_y| > k_{y,max}$ , where  $k_{y,max}$  is the wave vector corresponding to the lower voxel size in the  $y$  direction. An inverse FT resulted in rotated ACFs sampled with anisotropic resolution and *sinc* interpolated along the  $y$  direction. For each angle  $\alpha$ , we determined the FWHM of the ACF along the high resolution,  $x$ , direction. In this way we calculated the angular dependence of the FWHM as determined from anisotropically sampled ACFs with the high sampling resolution always parallel to the FWHM direction. The resulting angular dependencies show that a lower resolution perpendicular to the FWHM direction significantly affects the estimate of the FWHM only away from the principal directions. We can thus obtain a high resolution estimate of the FWHM along a principal direction by anisotropically sampling data using some form of inner-volume imaging with reduced resolution perpendicular to that of the principal direction. The principal directions can be determined beforehand from a fast low resolution scan.

## RESULTS AND CONCLUSION

Since the primary goal of the proposed method is to detect orientational dependences of TB thickness we examined the effect of anisotropic sampling on the FWHM. A high resolution micro-CT scan of human trabecular bone (voxel size of  $(16\mu\text{m})^3$ ), was thresholded to obtain a baseline image. The matrix size of the image was  $250 \times 250 \times 250$ . The baseline TB structure was dilated by some number of voxels to simulate a change in trabecular thickness. This image was then convolved with a Gaussian ( $\sigma=1$  voxel) to account for partial volume effects present even in micro-CT images. The FT of this image was then zero filled, similarly as above, to simulate a lower scan resolution in the  $y$ - $z$  plane. Complex white noise was added in the non-zero region of the FT. The inverse FT then produced a noisy, anisotropically sampled image, *sinc*-interpolated in the lower resolution,  $y$ - $z$  plane (the matrix size was the same as in the initial image). Subsequently, the FWHM along the high resolution,  $x$ , direction was determined for various  $y$ - $z$  plane resolutions and various dilations of the trabeculae. The linear  $y$ - $z$  plane resolution was decreased by a factor of 2, 4, 8, 16 and 32. An incidental advantage of the anisotropic sampling is an increase in signal to noise ratio (SNR) due to the increased voxel size at lower  $y$ - $z$  plane resolutions. The noise amplitude was chosen such that for the highest resolution image the SNR was smaller than 1 and trabeculae could not be discerned in the image. As Fig. 2a) shows, at that resolution changes in trabecular thickness could still be detected albeit with significant noise. This surprising result is a consequence of the robustness of the ACF to noise. In a noisy image the main noise contribution to the ACF is the autocorrelation of the noise which is a delta function at the center of image space. This feature can easily be removed by quadratic interpolation of the ACF at the center of image space, as was done in our simulations. In accordance with Fig. 1 the thickness estimate increases at lower resolutions since we did not choose a principal direction for the high resolution,  $x$ , FWHM direction. Nevertheless, there is a clear linear dependence between the FWHM and the number of dilations (thickness) at all resolutions, with slopes 0.51, 0.63, 0.56, 0.53, 0.51, 0.38 and 0.35 corresponding to the noiseless and noisy image with 0, 2, 4, 8, 16 and 32 times lowered linear  $y$ - $z$  resolution, respectively. We see (Fig.2), that the 8x lowered resolution offers a "sweet spot" with significant,  $8^2$ , acquisition-time gains at a sensitivity and even accuracy close to that of the noiseless image. As a way to measure the principal values of the thickness anisotropy tensor, we thus propose a fast autocorrelation anisotropic readout (FAAR) acquisition along the principal directions of the anisotropy tensor as determined by a lower resolution scan. This method offers great promise for high resolution in-vivo measurements of trabecular bone thickness and anisotropy.

[1] C. H. Turner, J. Biomech. 25: 1-9, 1992; [2] S. N. Hwang et al, Med Phys. 24: 1255, 1997; [3] C. A. Barrall et al, Science 255: 714-717, 1992;

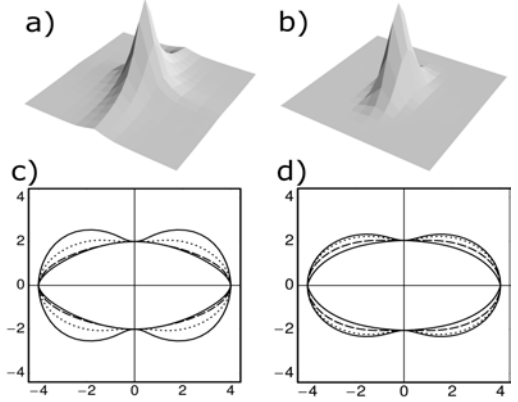


Figure 1. a) Lorentzian and b) Gaussian product ACF. Polar plots of FWHM estimates (in pixels) for c) Lorentzian and d) Gaussian product ACFs at various levels of anisotropy. Inner solid line corresponds to highest, isotropic resolution. Dashed/dotted line corresponds to halved/quartered  $y$  resolution. The outer solid line corresponds to an 8x larger voxel size in  $y$ .

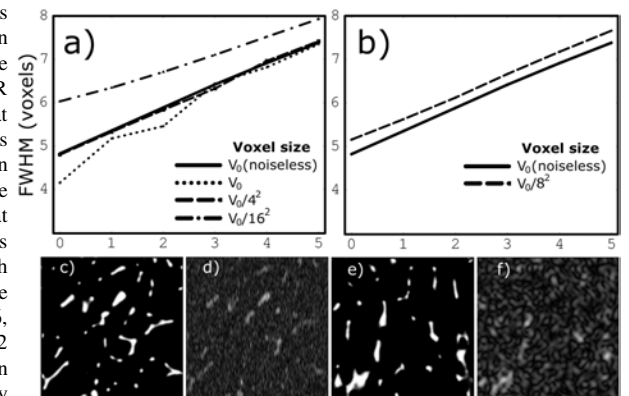


Figure 2. a) and b) FWHM estimates along the high resolution direction for various  $y$ - $z$  plane resolutions as a function of the number of dilations. c)  $x$ - $y$  (perpendicular to the bone's axis) and e)  $y$ - $z$  (parallel to the bone's axis) slices of the noiseless high resolution image. d) and e) corresponding slices in the noisy image with the linear  $y$ - $z$  resolution reduced by a factor of 8.